

Dispersion Coalescence: Kinetic Stability of Creamed Dispersions

Lloyd Lobo, Ivan Ivanov, and Darsh Wasan

Dept. of Chemical Engineering, Illinois Institute of Technology, Chicago, IL 60616

A model is developed to predict the coalescence behavior in liquid-liquid dispersions. Coalescence times are based on the lifetimes of the single films that are formed between adjoining drops in a creamed or sedimented dispersion. The model is developed for smaller drop sized dispersions ($< 100 \mu\text{m}$) in which the drops are not substantially deformed due to gravitational forces. The model predicts that coalescence occurs between the emulsion drops without the gross separation of the dispersed phase (that is, the dispersion does not separate into distinct oil and water phases). As a result of interdrop coalescence, the mean drop size of the dispersed phase increases along with an increase in the polydispersity of the drop size. The model's predictions are used to develop a quantitative relationship between the lifetime of the single film and the rate of increase of the mean drop size of the dispersion. The model also accounts for the effect of surfactant on dispersion stability via the models of single film drainage in the presence of surfactant.

Introduction

Liquid-liquid dispersions or emulsions exist in a wide variety of products as well as chemical processes. In the chemical industry, emulsions are commonly encountered in solvent extraction processes and in the petroleum industry. Several commercial products, such as paints, foods, and cosmetics are dispersions, either of the oil-in-water type or the water-in-oil type. In most cases, these dispersions are stabilized by surface active materials. Dispersions in which the drop sizes are large, undergo creaming or sedimentation of the disperse phase (due to the gravitational force) and, in order for these products to exhibit long shelf lives, these creams are expected to exhibit stability against the coalescence of the drops. Since in most of commercial emulsion type products, the drop size of the disperse phase is one of the major factors that determine the quality and functionality of the product, it is important to develop a mathematical model in order to predict the change in the drop size of the dispersions while they are on the shelf or in storage.

Figure 1 shows a typical dispersion of the oil-in-water type, which has creamed. The dispersion in the container shows three distinct regions. At the bottom is a clear continuous aqueous

phase which contains the surfactant; in the middle is the cream, which is a concentrated dispersion formed due to the buoyancy of oil drops and the top phase is a clear oil phase which is formed by the coalescence of the oil drops at the top. Coalescence can take place between the oil drops and the clear oil phase at the top of the cream, in which case the height of the clear oil phase increases while the height of the cream decreases; and/or between the oil drops themselves, in which case the mean drop size in the cream increases. Figure 1 in this article, as well as the subsequent mathematical treatment, is developed for oil-in-water emulsions. However, this mathematical treatment is exactly applicable for the water-in-oil emulsions, which can be visualized by turning Figure 1 over.

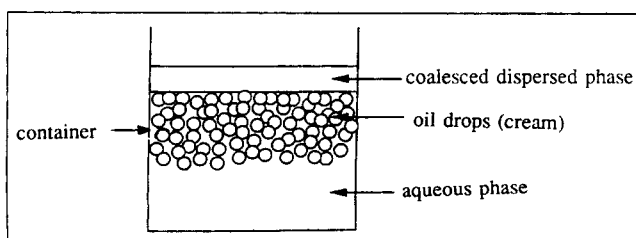


Figure 1. Oil-in-water type creamed dispersion.

Correspondence concerning this article should be addressed to Darsh Wasan.

Present address of Ivan Ivanov: Lab. of Thermodynamics and Physico-chemical Hydrodynamics, Faculty of Chemistry, University of Sofia, 1126 Sofia, Bulgaria.

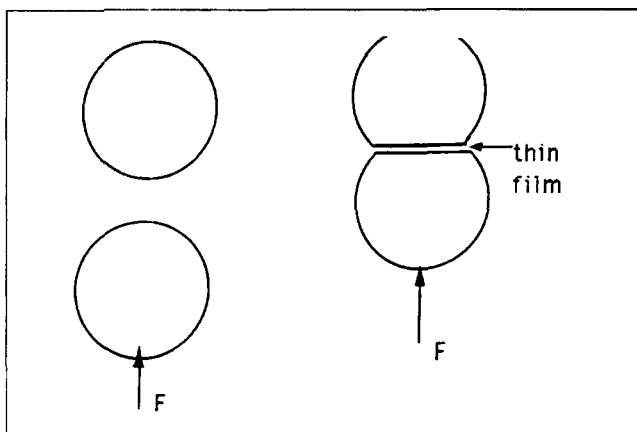


Figure 2. Thin film formed between two approaching drops.

Within the cream, the drops are in close proximity with each other and the coalescence of these drops is governed by the stability of the thin film that is formed between two drops. Figure 2 shows two drops approaching each other. When the distance between the drops is less than $1 \mu\text{m}$, their interfaces interact hydrodynamically and begin to deform. The various stages of deformation have been discussed by Ivanov and Dimitrov (1988). In the final stage, the interfaces deform to form a plane parallel thin film and they showed that the drainage and rupture of the plane parallel film is the rate controlling step in the overall process. The stability of thin plane parallel films has been analyzed extensively with respect to film drainage and rupture and several investigators have studied the effect of surfactant on film stability, with the most recent of these being Ivanov (1980), Traykov and Ivanov (1977), and Ivanov et al. (1985), as well as Zapryanov et al. (1983), and Malhotra and Wasan (1985). Their models use measurable bulk and surface properties (in the presence of surfactant) such as viscosity, interfacial shear and dilational viscosity, surface and bulk surfactant diffusivity, and so on to predict the drainage and lifetime of the films. The agreement of these models with experimental data was found to be quite good. However, up to now, the relation between the lifetime of single films and dispersion stability has been mainly empirical or mechanistic. Hartland and Vohra (1980) and Hartland and Gakis (1979) were the first to attempt a model that relates the lifetime of single films to dispersion stability. Their treatment was for fairly large drop sized dispersions (around 1 mm) in the absence of surfactant. In this study, we have extended their analysis to quantify the coalescence within creamed or sedimented dispersions with drop sizes less than $100 \mu\text{m}$ and also to account for the presence of surfactants, which are commonly used as stabilizers. The model is based on the lifetime of single films.

Coalescence of single bubbles

Consider two drops separated by a draining film. Figure 3a shows the configuration for two equal sized drops, in which case the film is planar. The drops are pressed against each other with a force F which, for the purpose of this analysis, is the buoyancy force.

Assuming that there is no deformation of the drop due to gravity, the surface of the drop that does not form part of the

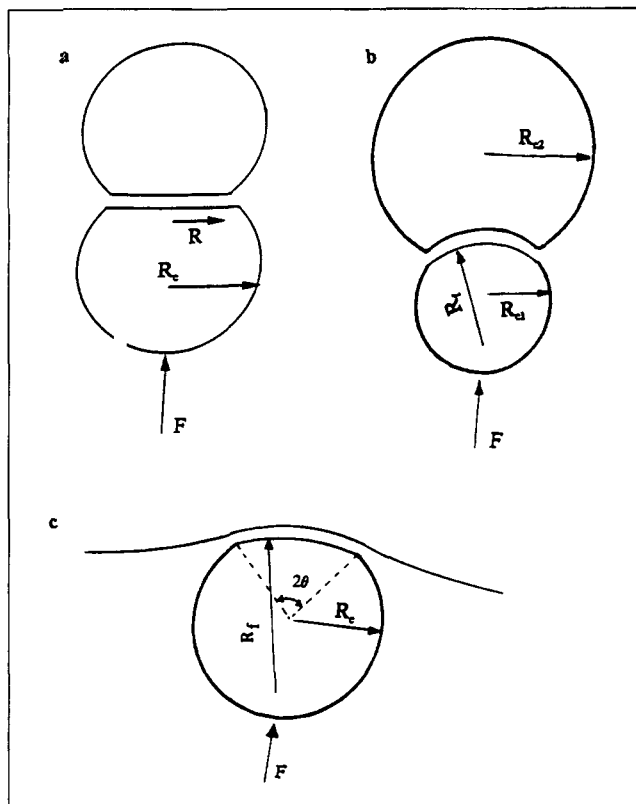


Figure 3. Films formed by (a) even sized drops, (b) uneven sized drops, and (c) a drop in contact with its bulk homophase.

film is spherical, and the capillary pressure P_g (excess pressure in the drop over that in the bulk liquid) is given by:

$$P_g = \frac{2\sigma}{R_c} \quad (1)$$

Since the pressure jump across a flat surface is zero, the pressure in the film equals that in the drop and

$$P_f = P_g = \frac{2\sigma}{R_c} \quad (2)$$

From the force balance on the drop:

$$P_f A_f = F \quad (3)$$

where A_f is the area of the film (πR^2).

Substituting Eq. 2 in Eq. 3 and using the buoyancy force for $F = 4/3\pi R_c^3 \Delta\rho g$ we obtain the radius of the film as:

$$R^2 = \frac{2}{3} R_c^4 \frac{\Delta\rho g}{\sigma} = \frac{2}{3} R_c^4 b \quad (4)$$

where

$$b = \frac{\Delta\rho g}{\sigma}$$

$R_c^2 b$ is called the Eötvös number and represents the ratio of the gravitational forces to the capillary forces.

For two drops of unequal size, R_{c1} and R_{c2} , shown in Figure 3b, the film is always curved and the radius of curvature of the film, R_f , is given by:

$$R_f = \frac{2R_{c1} R_{c2}}{R_{c1} - R_{c2}} \quad (5)$$

The area of the film, A_f' , projected normal to the line of centers of the drop is given by

$$A_f' = \frac{F}{\sigma} \left[\frac{R_{c1} R_{c2}}{R_{c1} + R_{c2}} \right] \quad (6)$$

In the limiting case the radius of the drop $R_{c2} = \infty$ and the lower drop is in contact with its homophase, as shown in Figure 3c. Equations 5 and 6 are transformed to:

$$R_f = 2R_c \quad (7)$$

and

$$A_f' = \frac{F}{\sigma} R_c \quad (8)$$

The above equations define the geometrical relations for the films of monodisperse and polydisperse drop systems. Strictly speaking, they are valid in the absence of disjoining pressure, but are good approximations even in this case.

Film drainage and rupture

There are many models (Frankel and Mysels, 1962; Hodgson and Woods, 1969; Charles and Mason, 1960; Burill and Woods, 1969, 1973) for predicting rates of film thinning based on the interfacial properties. The first mathematical analysis was the Reynolds parallel disk model (Reynolds, 1881). In this case, the film is modeled to be the liquid between two solid parallel discs (of radius R) pressed together by a force F and the rate of drainage is given by:

$$V_{RE} = \frac{2h^3 F}{3\pi\mu R^4} \quad (9)$$

This model represents a conservative prediction of the rate of film drainage since it assumes that the fluid interfaces are immobile, or solid like, and dimple formation is neglected.

In the first approach for our model, the films in the cream are assumed to drain according to Reynolds equation. The initial thickness of the film is assumed to be infinity, ∞ , and, as the film drains, the thickness decreases to some critical value h_{cr} at which point it will rupture. The lifetime of the film is given by

$$\tau = \int_{\infty}^{h_{cr}} -\frac{dh}{V_{RE}} = \frac{3}{4\pi} \frac{\mu A_f'^2}{F h_{cr}^2} = \frac{3\pi\mu R^4}{4h_{cr}^2 F} = \frac{3}{16\pi} \frac{\mu R_c^2}{\sigma^2 h_{cr}^2} F \quad (10)$$

The critical thickness of the films is obtained by calculating the thickness of the film at which the local fluctuations of

thermal capillary waves becomes unstable (Maldarelli and Jain, 1981; Scheludko, 1967; Vrij, 1966). Ivanov (1980) concludes, from experimental data available in literature, that h_{cr} has a value of about 25–40 nm for large films (0.1 mm) and the small variations of the value of the critical thickness from system to system make little or no difference to the lifetime of drops (Eq. 10), which is determined mostly by the variations in the velocity of thinning or in the drainage rate. It is assumed, in this study, that this finding is also true for smaller drops ($R_c < 50 \mu\text{m}$). It is interesting to observe the relationship between the applied force and the film lifetime in Eq. 10; τ increases with the applied force at a fixed drop size R_c . The reason for this is due to the increase in the film area caused by the increase in the applied force (Eqs. 3 and 8). As a consequence of this result it is easily shown that due to larger buoyancy forces large drops are more stable than smaller drops.

Model Development

Model geometry

In order to obtain a realistic model for the coalescence in the dispersion, it is necessary to choose a geometric arrangement of the drops in the creamed or sedimented dispersion that is close to reality. Hartland and Vohra (1980) and Hartland and Gakis (1979) have developed a model to quantify the stability of creamed emulsions (which they refer to as batch emulsions), for larger sized drops ($> 1 \text{ mm}$), based on single film stability. The geometry they chose was a simple cubic packing in which horizontal layers of drops, which are highly deformed, are stacked vertically above each other. The results of their analysis showed that coalescence only occurred at the interface between the creamed emulsion drops and the coalesced bulk dispersed phase. Thus, while the height of the dispersion decreases with time, the size of the drops within the emulsion remains the same. Because the drop sizes of interest to us in this study are much smaller ($< 100 \mu\text{m}$), it is unrealistic to assume, as they did, large deformations in the drops since the capillary forces dominate over the gravitational forces and the drops are not easily deformable. Consequently, the vertical stack arrangement is also unrealistic because the drops, in order to minimize deformation, will occupy a lattice in which their free energy is minimized.

The geometrical lattice assumed in this model is shown in Figure 4. This is commonly known as body centered cubic. In order to simplify the analysis, the stack is assumed to be two-dimensional in this study. This translates the spherical drops into cylindrical rods or discs whose width into the plane of the article is unity, and they are free to move about within the plane. The consequence of this assumption is that the absolute

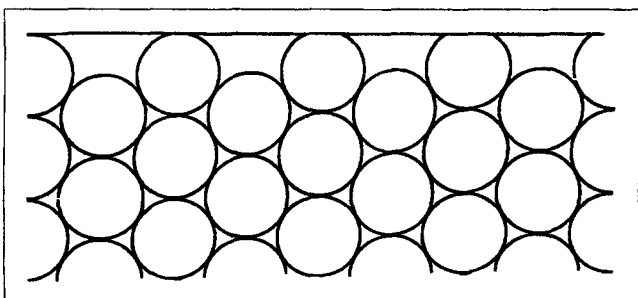


Figure 4. Close packed spheres in a cream.

scale of the coalescence times would be different from the 3-Dimensional case. However, the analysis would help in understanding of the problem because the coalescence sequence and the trends are expected to be similar to the 3-Dimensional case. A semi-empirical extension of the results of the 2-D model to the 3-D model is presented at the end of the article.

In the geometrical configuration shown in Figure 4, each drop is supported from above by two drops while being pushed from below by two drops. If the deformation of the drops is high, each drop will be in contact with two additional drops, one vertically above and one vertically below the drop. As shown below, the deformation in the stack can be neglected, and the presence of these two drops can be neglected.

Deformation of the drops due to multiple films

Within the bulk dispersion, each drop is in contact with more than one film (in this packing it is 4). The main question or difficulty that arises when analyzing this problem is how two or more films, in contact with a single drop, interact with each other. The film can 'feel' the presence of another film through the change in the capillary pressure within the drop. The change in the capillary pressure is directly related to the deviation from sphericity of the surface of the drop that does not form part of the films. Thus, it is necessary to determine the magnitude of the deformation of the drop surfaces in order to determine the degree of interaction between the films on each drop. If this deformation is substantial, the change in the capillary pressure has to be determined by the numerical integration of the Laplace equation for the drop surface [similar to the procedure employed by Hartland and Vohra (1980)] and the procedure will have to be done for each drop. This procedure involves a large amount of computation but, if the deformations are small, can be avoided.

The degree of deformation can be determined by considering a single drop in a vertical stack of drops. The drop has the two films diametrically opposite each other, and the error involved in neglecting the deformation can be evaluated in two ways: by determining the change in the capillary pressure when the condition of constant drop volume is imposed and by determining the error (or changing) in the volume of the drop if constant capillary pressure is assumed. If these errors are small the deformation can be safely neglected. The method of calculating these errors is presented in the Appendix. The results from these analyses show that the percent change in the capillary pressure is quite low (< 5%) for emulsions with drop sizes of interest to us. The example discussed in the Appendix shows that the maximum change in the capillary pressure is less than 2% for a typical emulsion ($\Delta\rho = 0.2 \text{ gm/cm}^3$, $\sigma = 5 \text{ dyne/cm}$) of drop size, $R_c = 50 \text{ }\mu\text{m}$ and a cream height of 6 cm. This height is more or less typical to many commercial products and since this deformation is evaluated to be small, we further neglect this effect, which signifies that the films are independent of each other.

Assumptions used in the model

1. The stack of the drops is two-dimensional. The drops are actually discs—infinite in extent but assumed to be with a width of unity in the plane of the paper.

Hartland and Vohra (1980) have derived the film drainage equations for two-dimensional drops. For planar films the

lifetime τ is given by:

$$\tau = \frac{\mu A_f^3}{2F h_{cr}^2} \quad (11)$$

where

$$A_f = \frac{FR_c}{\sigma}$$

For curved films, formed between drops of size R_{c1} and R_{c2} , we have:

$$\tau = \frac{12\mu R_f^3}{h_{cr}^2 F} (\sin\theta - \theta\cos\theta) \quad (12)$$

where

$$R_f = 2 \left(\frac{R_{c1} R_{c2}}{R_{c1} - R_{c2}} \right)$$

and happens to be the same as Eq. 5, and θ is half the angle subtended by the arc of the curved film (See Figure 3b).

2. All the films rupture at the same critical thickness, and the lifetime of the film is only a function of the drop size and the force, as shown in Eqs. 11 and 12.

3. The initial condition is shown in Figure 4. All the drops have the same size and, having settled instantaneously, at $t=0$ all the films have the same initial thickness which is assumed to be infinity for the purpose of calculating the film lifetime according to Eqs. 11 and 12. We also assume that initially there is a layer of the coalesced dispersed phase at the top of the cream.

4. The surfaces of the drops which do not form parts of the films are parts of spheres (nondeformed) and the change in the volume of the drops due to the films is neglected. As shown in the Appendix, the maximum error in this assumption is less than 2% when the height of the batch dispersion is about 6 cm. This assumption simplifies the calculation of film lifetimes because each of the films can be treated independently.

5. The Reynolds equation (Eq. 9) is used to describe the film drainage rate. As stated before, the model assumes immobile surfaces. Fluid films containing adsorbed surfactants have, however, partially mobile surfaces. Ivanov (1980) showed that the effect of surfactant can be accounted for by a mobility factor, M , in the film drainage equation. The mobility factor is related to the mobility of the surfaces of the draining film in the presence of surfactant.

$$\frac{V}{V_{RE}} = M \quad (13)$$

The effect of surfactant and partial surface mobility on dispersion stability is evaluated later in this article.

6. The thermodynamic interactions between the film surfaces are neglected. In this case, the driving force for drainage is the pressure difference, ΔP , between the film and the bulk solution and it is given by:

$$\Delta P = P_f = \frac{F}{A_f} \quad (14)$$

The velocity of drainage V_{RE} is a function of the driving force and is given by:

$$V_{RE} = \frac{h^3}{\mu A_f^2} \Delta P \quad (15)$$

In the case where the film surfaces interact with each other, the interactions, accounted for by the disjoining pressure, Π , oppose the draining of the film, and

$$\Delta P = \frac{F}{A_f} - \Pi \quad (16)$$

7. The film drainage is not influenced by the drainage in the Plateau borders.

Procedure for calculating the coalescence sequence and times

From Eq. 11 it is seen that the lifetime of the film τ is proportional to F^2 (for the 2-D drops) which implies that the drops with the shortest lifetime are the ones with the smallest buoyancy force acting on them, that is, the films at the bottom of the stack. Hence, the bottom two rows of drops will coalesce first within a time, τ_1 , which is the lifetime of the films between the two rows of drops. All subsequent coalescence times are normalized with respect to τ_1 .

Force Balance on a Single Drop. Each drop in the array is in contact with 4 or less drops, as shown in Figure 5, and the force balance is given by:

$$\begin{aligned} F_1 \cos \phi_1 + F_2 \cos \phi_2 + w &= F'_1 \cos \phi'_1 + F'_2 \cos \phi'_2 \\ F_1 \sin \phi_1 + F'_2 \sin \phi'_2 &= F'_1 \sin \phi'_1 + F_2 \sin \phi_2 \end{aligned} \quad (17)$$

The forces, F , and the angles, ϕ , are defined in Figure 5, w is the buoyant weight of the drop.

These equations are general for any drop at any time of the dispersion life. Initially the drops are all equal sized with sym-

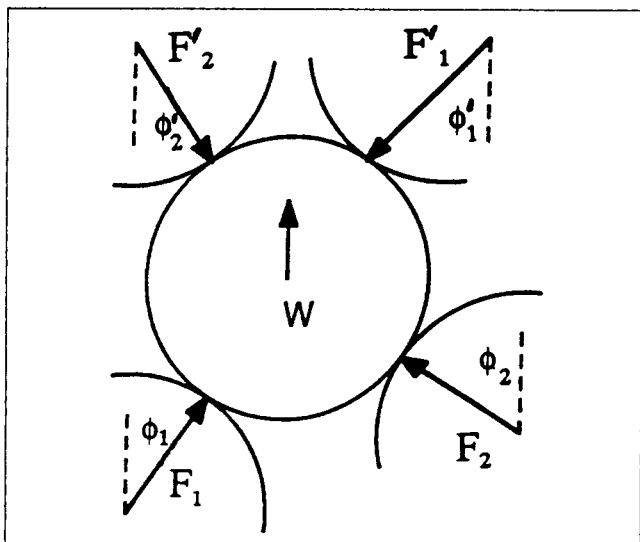


Figure 5. Forces acting on a single drop in a stack.

metrical forces and equal angles. At later stages, due to coalescence, all the drops are not equal and, therefore, the geometrical symmetry is disrupted and the angles are not equal and the forces are not symmetrical. The angles are calculated from the geometry of the stack and the forces are obtained by making the force balance (Eq. 17) from the bottom of the stack and working up to the top.

Sequence of Coalescence. By using the forces on the films and the sizes of the parent drops, the lifetime of all the films in the stack are determined from Eqs. 11 and 12. The films having the shortest lifetime will rupture and the drops adjoining those films will coalesce. If two films on the same drop have the same lifetime, the coalescence is assumed to occur in such a way that the symmetry of the lattice is preserved. For example, in Figure 6 all the films which are marked (in 6a) have the same lifetime and, due to random coalescence, different resulting configurations are possible (Figure 6b-6d). Figure 6b is the configuration with the maximum symmetry and the model assumes that the coalescence of the films in Figures 6a results in the configuration in Figure 6b.

Film Age. Since the coalescence starts at the bottom layers, it is fairly apparent that the drops at the top and their films are not distributed by the coalescence. Consequently, these films are continuously draining through the different coalescence steps. Any film that is formed from a newly created drop or as a consequence or rearrangement of the drops in the

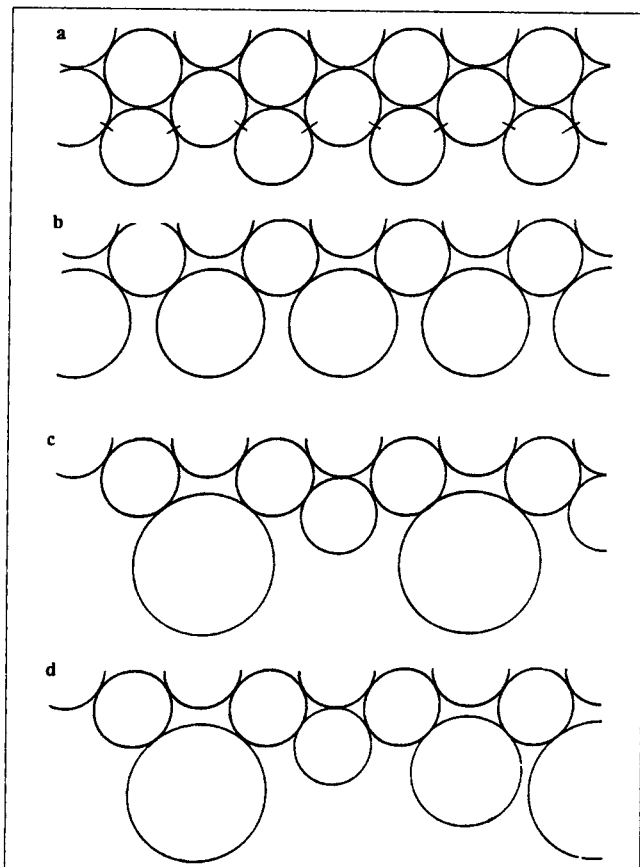


Figure 6. Possible configurations of drops (b-d) resulting from rupture of films having the same lifetime, (a).

lattice is considered to be a new film. The birth time of the new film is at the time of formation/rearrangement of the parent drop and its thickness at birth is assumed to be infinity. All other films which are not disturbed are considered to be old films and the drainage histories of these are accounted for.

Even though the old films are not distributed, the forces on them may change due to coalescence or rearrangement of drops in the stack below the parent drops and thus change their drainage rates. Since the capillary pressure (which is specified by the size of the parent drops of the film) on the old film does not change, the lifetime of the film is only a function of the force, $[\tau = \tau(F)]$, as shown in Eqs. 11 and 12.

Consider an old film at the end of m coalescence steps, during which parent drops haven't moved or coalesced. The film has drained during these m preceding steps under the influence of varying forces acting on the film. If the time between the i th and $(i+1)$ th coalescence steps is t_i , and if the force acting on the film during this time period is F_i , the fractional decrease in the lifetime on the drop, τ_f , during the i th step is given by:

$$\tau_f(i) = \frac{t_i}{\tau(F_i)} \quad (18)$$

The fraction of the film lifetime that has decreased due to drainage, after m steps, is obtained by adding the fractional drainage for the m preceding steps. The remainder of the lifetime of the film after m coalescence steps, τ_m , is given by:

$$\tau_m = \left[1 - \sum_{i=0}^m \frac{t_i}{\tau(F_i)} \right] \tau(F_m) \quad (19)$$

where $\tau(F_i)$ and $\tau(F_m)$ are given by Eqs. 11 or 12.

Thus, at any coalescence step the lifetimes of all the new films and the old films are evaluated and compared and the film with the shortest lifetime is assumed to rupture.

Rearrangement. Due to the fact that coalescence starts from the bottom of the stack, the drop size increases at the bottom. When two rows of two-dimensional drops of radii R_{c1} and R_{c2} , respectively, coalesce, the resultant row will have drops with a radius R_{cr} given by:

$$R_{cr} = \sqrt{R_{c1}^2 + R_{c2}^2} \quad (20)$$

This process will continue until, at some point, the value of R_{cr} will become too large for the drops to be accommodated within a single row without significant deformation. Consequently, the new drops, in order to minimize deformation, will redistribute themselves into two rows, as shown in Figure 7.

At each step, the force balance is made for each film (Eq. 17). By knowing the size of the parent drops and the force acting on each film, we can calculate the lifetime of each film while, at the same time taking into account the film age and fractional lifetimes, as discussed above. The lifetime of all of the films are compared and the drops adjacent to the film(s) with the shortest lifetime are assumed to coalesce after the time, equal to this lifetime, has elapsed. After coalescence we use the rules stated above (rearrangement and stack symmetry) to determine the new geometry of the stack. The force balance is then repeated for the new geometry and the film lifetimes

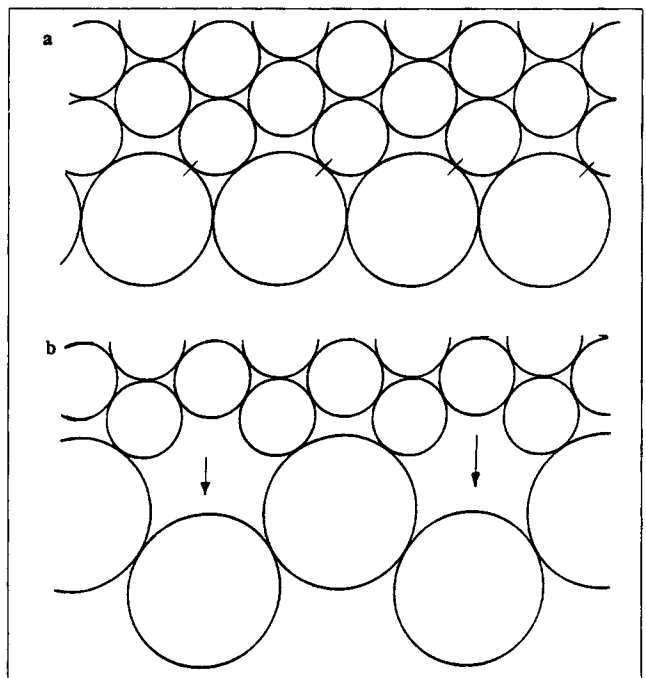


Figure 7. Rearrangement of drops which are formed due to rupture of the films (a).

are calculated again to determine the next coalescence step. The procedure is repeated to obtain successive coalescence steps and their relative times of occurring.

Results

To observe the sequence of coalescence, a 20 layered stack of drops was analyzed. At the initial stage, the dispersion is monodisperse and the cream consists of drops arranged in a close-packed hexagonal structure, as shown in Figure 4. Figure 8 shows some of the stages of coalescence along with the relative coalescence times. The coalescence times are relative to the time τ_1 . From Figure 8 we see that the model predicts that coalescence occurs between the drops in the cream and not at

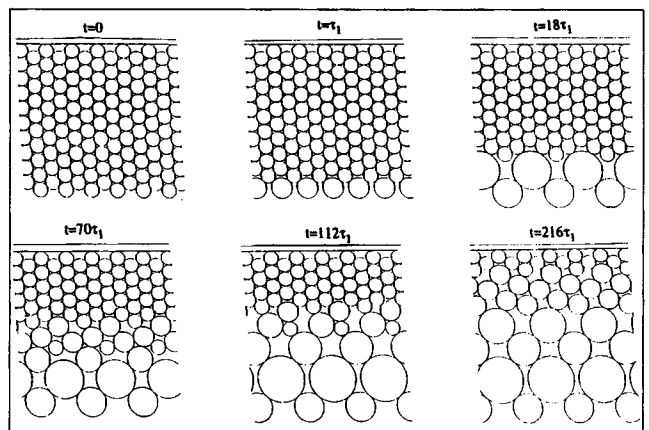


Figure 8. Sequence of coalescence within a cream along with respective times of occurring.

the top interface between the bulk aqueous and oil phases. Thus, while the height of the cream remains constant, interdrop coalescence results in the change of the mean drop size and the initial monodispersed emulsion becomes polydisperse with the polydispersity increasing with time.

Following are some of the observations that can be drawn from the coalescence analysis and Figure 8:

- The coalescence starts with the drops at the bottom of the stack and, later, it also takes place in the middle.
- The polydispersity of the cream increases with time.
- The mean drop size increases with time.
- The height of the cream remains almost constant.

These results are very different from those obtained by Hartland and Vohra (1980) and Hartland and Gakis (1979) in their model for large drop-size creams. The reason for the difference between the results of the two models is due to different drop-size ranges for which the two models are applicable. Specifically, the differences are due to the large deformation of the larger drop-sized dispersions studied in their models, as compared to our model where the deformations are neglected. In reality, emulsions are polydisperse and in many of these systems, some of the drops can be large enough to be deformed substantially, while others are small enough for the capillary forces to minimize deformation. In these systems, the coalescence characteristics will be in between those predicted by the two models- where coalescence will occur throughout the stack.

Another important point to note is that the model always assumes that the capillary forces exceed the gravity forces and deformation is negligible, as shown in the Appendix. While this may be true for the initial monodispersed stack (with small drops), as the coalescence proceeds, the drops at the bottom of the stack can become large enough to be substantially deformed and violate this assumption, therefore changing the coalescence characteristics. Also, under certain conditions, the buoyancy force of the large drops at the bottom of the stack may be large enough for those drops to push their way from the bottom of the stack to the top. In both situations, the present model will fail to predict the coalescence behavior. The model is, however, useful for characterizing the initial stages of coalescence in which the drops sizes are fairly small.

Development of a coalescence equation

From the results of the coalescence model, it is possible to develop a simple, quantitative relationship, or equation, that can predict the coalescence in the cream from the system parameters such as drop size, interfacial tension, and so on. This coalescence equation can be used to estimate the change in the drop size of the cream as a function of time. The results of the model show that the coalescence process starts at the lowest layers and propagates through the upper layers. The mean drop size within the layers which have undergone coalescence also changes (increases) during the process. Thus, in order to completely characterize the drop size in the cream, one needs to know the rate at which the coalescence propagates upwards and the mean drop size within the coalesced layers. Figure 9 shows the time at which the drops in a given numbered layer, n , undergo coalescence. The time in Figure 9 is normalized with respect to τ_1 , similar to the times shown in Figure 8. The layers of drops above the layer n , remain unchanged from the initial condition, that is, all the drops are monodispersed with

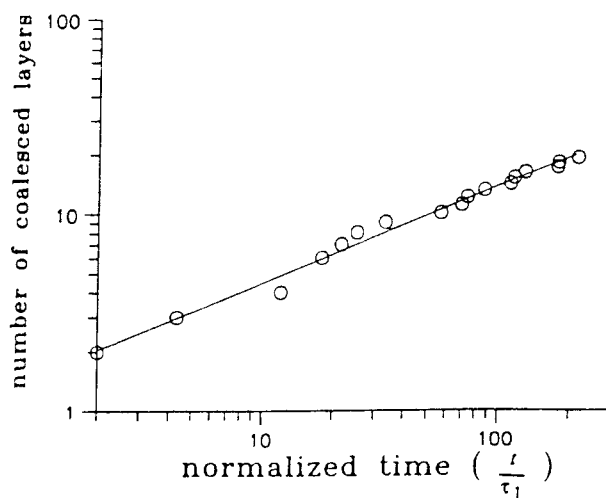


Figure 9. Rate at which the coalescence process moves upward through the stack of drops.

the same initial size. Figure 10 shows the arithmetic mean drop size within the coalesced layers as the coalescence process moves upwards through each numbered layer. Thus, in order to determine the mean drop size within the coalesced layers at any time, t , one should use Figure 9 to determine the number of the original layers which have undergone coalescence and use Figure 10 to determine the mean drop size within these coalesced layers. Figures 9 and 10 can be also used to determine the mean drop size, within the entire cream, at any time. For example, after a time equal to $18\tau_1$, the number of the initial layers that have coalesced is 6 (see Figure 8) and the arithmetic mean drop size within these coalesced layers is $1.88d_i$, where d_i is the initial drop diameter. Since the mean drop size in the remaining 14 layers is d_i , the mean drop size of the entire cream can be determined. It should also be noted that since the coalescence starts from the bottom, the coalescence sequence and times are independent of the total height of the cream.

From Figures 9 and 10 it is possible to observe some trend in the coalescence process and develop a usable analytical solution to predict the change in the drop size within a cream after a given time. Figure 9 shows that the rate of coalescence of the layers can be expressed as a power function of the

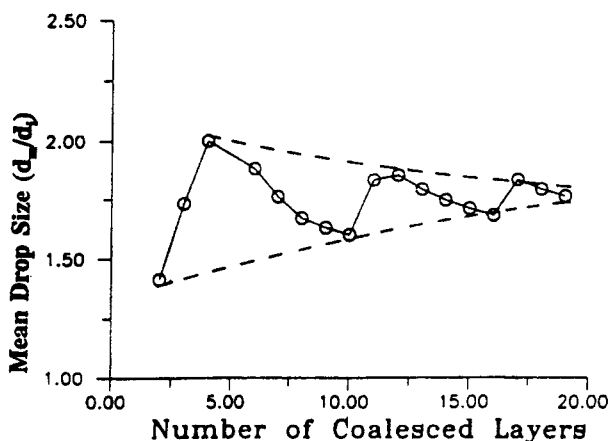


Figure 10. Mean drop size within the layers that have coalesced.

normalized time. The number of original layers, n , which has coalesced after normalized time, t/τ_1 , is given by:

$$n = 1.46 \left(\frac{t}{\tau_1} \right)^{0.48} \quad (21)$$

The computations show that the variation in the arithmetic mean drop size with the number of coalesced layers (Figure 10) is oscillatory, with the amplitude of the oscillations decreasing as the number of coalesced layers increases. The reason for the oscillations is due to there being fewer drops in the coalesced layers at the initial stages, since the arithmetic mean drop size is very sensitive to the total number of drops. As the coalescence process evolves, the number of drops in the coalesced layers increases, the changes in the mean drop sizes are not as sharp and, eventually, the mean drop size is expected to reach some steady value. By extrapolating the curve (using the dashed lines) in Figure 10 to a large number of coalesced layers, the arithmetic mean drop size, d_m , within the coalesced layers can be approximated by

$$d_m \approx 1.78d_i \quad (22)$$

From Eqs. 21 and 22 we can estimate the change in the mean drop size within a batch dispersion or cream. By using a volume balance on the dispersed phase, the arithmetic mean drop size, \bar{d} , of a cream of initial drop size, d_i , and height, H_{cr} , any time, t , is obtained as:

$$\bar{d} = d_i \left(\frac{1.78\lambda + 1}{\lambda + 1} \right) \quad (23)$$

where

$$\lambda = \frac{1.46 \left(\frac{t}{\tau_1} \right)^{0.48}}{1.78^2} \left(\frac{H_{cr}}{r_i} - 1 \right) - 1.46 \left(\frac{t}{\tau_1} \right)^{0.48} \quad (24)$$

Effect of surfactant of film and dispersion stability

In the case of fluid films containing surfactant, the films are not completely immobile but have a partial mobility. As mentioned before, in this case the Reynolds equation is not valid. Ivanov and Traykov (1976) derived that the velocity of drainage, in the presence of surfactant, is given by:

$$V = V_{RE} \left(1 + b_s + \frac{h_s}{h} \right) \quad (25)$$

The term in the parenthesis is the mobility factor, M . b_s and h_s are obtained from the surfactant properties by the following relationship:

$$b_s = \frac{3\mu D}{\Gamma \left(\frac{\partial \sigma_o}{\partial c_o} \right)} ; \quad h_s = \frac{6\mu D_s}{-\frac{\partial \sigma_o}{\partial \ln \Gamma_o}} \quad (26)$$

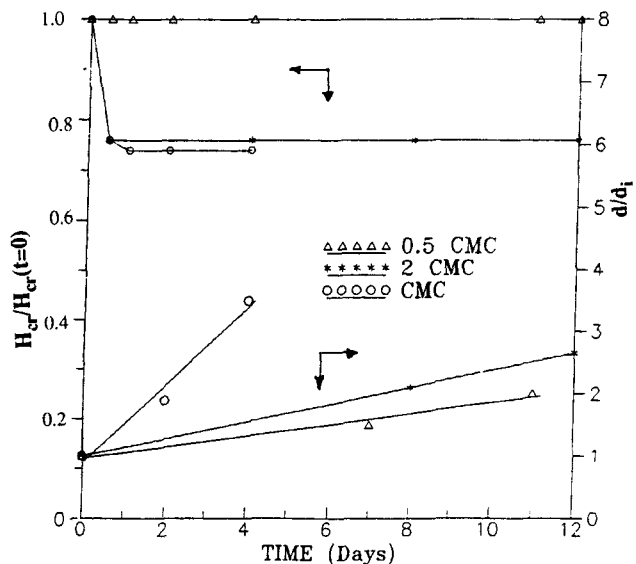


Figure 11. Coalescence behavior of a cream of hexadecane-in-water, stabilized by SDS.

where

Γ, c_s = surface and bulk concentrations of the surfactant
 D, D_s = surface and bulk diffusion coefficients of the surfactant
 o = equilibrium properties

If the disjoining pressure is small, the lifetime of the film is obtained by:

$$\tau = - \int_{\infty}^{h_{cr}} \frac{dh}{V} \quad (27)$$

Since the critical thickness of rupture has a minor influence on the lifetime of the film, Chakarova et al. (1990) obtained:

$$\tau = \frac{1}{L_o h_{cr} h_s} \left[1 - \frac{(1 + b_s) h_{cr}}{h_s} \ln \left[1 + \frac{h_s}{(1 + b_s) h_{cr}} \right] \right] \quad (28)$$

where $L_o = 2F/(3\pi\mu R^4)$. They found that the second term in the parenthesis is fairly invariable with surfactant concentration. Thus,

$$\tau = \frac{1}{L_o h_{cr} h_s} [1 + \text{constant}] \quad (29)$$

For two films having different radii, R_1 and R_2 , draining under different forces, F_1 and F_2 , the ratio of the lifetimes is given by:

$$\frac{\tau_2}{\tau_1} = \frac{L_{o1}}{L_{o2}} = \frac{F_1}{F_2} \left(\frac{R_1}{R_2} \right)^4 \quad (30)$$

because h_s is independent of F and R , and h_{cr} has only a small dependence on R . Thus, under these conditions (low surfactant concentration and low disjoining pressure) the ratio of the lifetimes has exactly the same relationship for the case when the Reynolds equation of film drainage was used (see Eq. 10), which means that this ratio is independent of surfactant concentration. Thus, the dependence of the relative coalescence

times on the number of the coalescing layer (Figure 9), calculated by our coalescence model, remains unchanged in the presence of surfactant. The effect of surfactant, in the coalescence equation, is to change the lifetime, τ_1 , of the first film, which indicates that surfactant basically scales the times of the coalescence steps, without changing the coalescence sequence. The lifetime τ_1 , in the presence of surfactant, can be determined from the Eq. 28.

Extension to 3-D systems

For the 2-D stack in the initial packed condition ($t=0$), the lifetime of the film as a function of its position, n , (it is actually the position of the lower parent drop) in the stack, is given by:

$$\tau_n = \tau_1 n^2 \quad ; \quad n = \left(\frac{\tau_n}{\tau_1} \right)^{0.5} \quad (31)$$

The equation is obtained by making the force balance on all the drops in the initial stack (see Figure 8 at $\tau=0$) and substituting the value of F into Eq. 11. Equation 31 yields the rate at which the coalescence process would propagate upward, through each layer, if the forces on each film remained the same as in the initial state. However, due to the rearrangement of drops and the redistribution of forces in the stack, at each coalescence step, the actual rate at which the coalescence propagates upwards does not follow this relation. The above equation can be written in the form:

$$n = k \left(\frac{t}{\tau_1} \right)^i \quad (32)$$

On comparing this equation with Eq. 21, we find that i is almost equal to 0.5 and the entire process is scaled by a factor k , which is greater than 1 (actually 1.46).

In the 3-D case, the geometrical factors are different, since each drop will be in contact with eight films. By following the same force balance for the 3-D case at the initial condition, along with the calculation of the film lifetimes (Eq. 10), the equivalent of Eq. 31 is given by:

$$\frac{\tau_n}{\tau_1} = n \quad (33)$$

The other factor that is needed is the mean drop size. For the 2-D case, the arithmetic mean drop size within the coalesced layers is approximately $1.78 d_i$ (Eq. 22) which represents a mean drop within the coalesced layers resulting from the coalescence of approximately 3 of the original drops.

If it is assumed that the coalescence sequence for the 3-D case is similar to the 2-D case, a similar relation as Eq. 32 can be arrived at for the 3-D case where the rate constant k has a value greater than 1 and the index, i , has a value close to 1. Similarly, if the mean drop (in the coalesced layers) for the 3-D case results from the coalescence of 3 original drops, then the average drop size in the coalesced layers, d_m , for the 3-D case is given by:

$$d_m = 1.5d_i \quad (34)$$

These two equations are sufficient to characterize the change in drop size, as a function of time. An equation, similar to Eq. 22, can be developed for the 3-D case, by using Eqs. 33 and 34.

$$\bar{d} = \frac{1.5\chi + 1}{\chi + 1} \quad (35)$$

where

$$\chi = \frac{\frac{k}{1.5^3} \left(\frac{t}{\tau_1} \right)^i}{\left(\frac{H_{cr}}{r_i} \right) - k \left(\frac{t}{\tau_1} \right)^i}$$

This extension of the results from the 2-D case to the 3-D case is an approximate and semiempirical one and a complete analysis should be made for the 3-D case in order to obtain exact values for k , i and d_m/d_i .

Experimental Results

In order to check the qualitative results of the model, experiments were made on the stability of dispersions of hexadecane-in-water emulsions. Sodium dodecyl sulfate was used as the surfactant. In order to minimize the effect of the disjoining pressure on the stability, the concentrations were chosen to be around the critical micelle concentration (cmc).

Emulsions were prepared by adding the oil phase, dropwise, into a stirred vessel containing the aqueous phase. The initial drop size was maintained around 20–30 μm and the volume of the dispersed phase was kept at 30%. After preparation, the emulsion drop size was measured using a photomicrographic technique (Menon and Wasan, 1984), and the arithmetic mean drop size was determined. The emulsion was then allowed to settle in a 2 cm diameter glass tube. Representative samples of the batch dispersion were taken out at different times and the mean drop size, \bar{d} was determined as a function of time.

Figure 11 shows the change in the mean drop size and height as a function of time. For two of the emulsions there was an initial decrease in the cream height, due to coalescence with the top bulk layer of oil. This was due to the presence of a few, relatively large drops in the polydisperse emulsion. After this initial decrease, the height of the dispersion did not change, while the mean drop size within the cream increased with time. These results imply that, in the smaller drop sized dispersions, coalescence occurs primarily between the drops in the cream, without the separation of a bulk oil phase. This result is also qualitatively predicted by the model. We would like to contrast these results with those of Hartland and Vohra (1978) for water-in-oil dispersions in the absence of any surfactant. The drop size of the emulsions was around 1mm, and they found that the height of the dispersion decreased with time without a change in the mean drop size occurring. In their systems, due to the large deformations of the larger-sized drops, the coalescence behavior is consistent with their model. In this study, our experiments have shown that for smaller drop-sized emulsions, the coalescence behavior cannot be predicted by their model and a more realistic treatment is the one presented in this study.

In this study, we make no attempt to compare the experimental results with the model predictions on a quantitative basis. The reason for this is because several of the model's assumptions cannot be realized by the experimental conditions, most notably the three-dimensional spherical drops and the polydispersity of the emulsions. Although an extension of the analysis is made for the 3-D case, it is still an approximate one, as mentioned above. The effect of polydispersity is more serious, since it would result in differential creaming (the larger drops creaming faster than the smaller drops) as well as results in a different packing configuration upon creaming. Princen (1986), Princen and Kiss (1987), and Princen (1990) discuss how the polydisperse emulsion systems cream and pack. From experiments, they found that the random packing of polydisperse systems (during creaming) is less efficient than the packing of monodisperse spheres. Other assumptions that are violated during the experiments are the finite creaming time and the effect of disjoining pressure (which could be quite large even around the cmc of the surfactant).

Effect of differential creaming

As stated earlier, for the initial condition of the cream it is assumed that all the drops have settled instantaneously with all the films having the same birth time. In reality, the initially well dispersed emulsion will take some finite time (greater than zero) to settle. In addition, the entire stack of drops do not form at the same time, but, the layers of drops will first stack at the top and the stack will increase in height by the addition of single layers of drops at a time. As a result of this differential creaming, the birth time of all the films will not be the same and, consequently, this could even change the coalescence sequence predicted by the model. While it is not feasible to determine all the possible sequences of coalescence, one can estimate the time of creaming and relate it to the applicability of the coalescence model described above.

The rate of creaming depends mainly on factors such as density difference of the two phases, drop size of the dispersed phase and viscosity of the continuous phase. Hartland and Jeelani (1988a,b), Jeelani and Hartland (1985), Jeelani et al. (1990), and Kumar and Hartland (1985) have developed mathematical models based on these physical parameters to determine the rate of creaming in batch dispersions. They assume the creaming dispersion consists of two zones: a sedimentation zone, where the drops have not yet formed films and a dense zone, where the drops are densely packed such as those shown in Figure 4. Kumar and Hartland (1985) obtained the relative velocity, u_s , of the drops in the sedimentation zone as:

$$u_s = \frac{\Delta\rho g (1 - \epsilon_s) d_i^2}{18 \mu (1 + 4.56\epsilon_s)} \quad (36)$$

where j is an index which is close to unity, ϵ_s is the volume fraction of the disperse phase in the sedimentation zone. The equation was derived from creaming data obtained at steady-state but is applicable to batch decay when the acceleration of the drops is small. Hartland and Jeelani (1988b) showed that the rate of shrinking of the sedimentation zone is given by:

$$-\frac{dx}{dt} = u_s (1 - \epsilon_s) \quad (37)$$

where x is the coordinate of the boundary of the sedimentation zone. When combining Eqs. 36 and 37, we obtain:

$$-\frac{dx}{dt} = \frac{\Delta\rho g (1 - \epsilon_s)^2 d_i^2}{18 \mu (1 + 4.56\epsilon_s)} \quad (38)$$

From experimental results, Jeelani et al. (1990) found that the disperse phase holdup in the sedimentation zone is a linear function of time, which is given by

$$\epsilon_s = \epsilon_o + \beta t \quad (39)$$

where β is an experimentally determined value.

The experimentally determined values of β were found to be small (0.005) and β was also found to decrease with drop diameter. Since their model was developed for relatively large drop sizes ($d_i > 500 \mu\text{m}$), the disperse phase holdup in the sedimentation zone can be assumed to be fairly invariant with time, for drop sizes less than $50 \mu\text{m}$, which are relevant to the coalescence model described above. In this case, Eq. 38 can be integrated to obtain the time for creaming, t_{cr} to get

$$t_{cr} = (H_{con} - H_{cr}) \left[\frac{18 \mu (1 + 4.56\epsilon_s)}{\Delta\rho g (1 - \epsilon_s)^2 d_i^2} \right] \quad (40)$$

H_{con} and H_{cr} , respectively, are the heights of the container and the cream after sedimentation is complete.

If the time for creaming is not much larger than the lifetime of the single film (τ_1), then the results obtained from the coalescence model would not differ substantially. For example, for an emulsion in which the drop diameter is $100 \mu\text{m}$ and the density difference is 0.2 g/cm^3 , the lifetime of the single film (τ_1) $\approx 100 \text{ s}$, as determined by the Reynold's equation (Eq. 9). If the oil phase fraction, ϵ_s , is around 30 vol. %, and the emulsion is taken in a 10 cm tall container ($H_{con} = 10 \text{ cm}$), the time for the entire creaming process to occur is about 700 s, which is approximately 7 times the lifetime for the single film. In Figure 8, it is seen that only the first three layers coalesce within a time of $7\tau_1$.

Thus, in this case the results of the coalescence model will not be substantially affected by the differential creaming. The ratio of the creaming time to the lifetime of single films will, however, increase with the decrease in the drop size (due to increase in t_{cr} and decrease in τ_1), and then the coalescence model will fail.

Conclusions

The model successfully bridges the relationship between the stability of films and the stability of creamed dispersions, and the relationships obtained by this mathematical treatment are valid with or without surfactant in the system. The model can be used (Eq. 23) to estimate the change in the mean drop size of the emulsion after a given time, by knowing the lifetime of a single film. Since the effect of added surfactant is only to scale the coalescence times, Eq. 23 can still be used to estimate the change in the mean drop size of the emulsion. The only change would be in the value of τ_1 in Eq. 24. τ_1 can be estimated from the single film drainage models, such as Eq. 28, which take into account the effect of surfactant. For the 3-D case, Eq. 35 can be used to estimate the change in the drop size, if the exact values of k and i are known.

The many assumptions listed above should, however, be kept in mind. The two major assumptions that could change the observed behavior from the predicted one are:

1. The films are born at the same instant. Normal creaming processes result in the top most layers forming the films first followed by the lower layers. The above assumption is valid if the time for creaming is much smaller than the lifetime of the initial films.

2. The effect of disjoining pressure is negligible. This assumption is only valid at low surfactant concentrations where the disjoining pressure does not substantially affect the drainage of the films.

In many cases (for example, in cosmetics products), the amount of surfactant is high enough for the thin films to be infinitely stable. This is caused by the high value of the disjoining pressure. In such circumstances, Hartland's model as well as the present model will not be applicable, since both these models are based on thin film stability. In these systems, the dispersion drops will cream to a close-packed configuration and remain stable. As all practical systems are inevitably polydisperse, the packing configuration will be different from Figure 4, as mentioned earlier and, for packing in such systems, one should refer to the works of Princen et al. cited earlier. In the case when the films are stable, polydispersity introduces another effect called Oswald ripening, whereby the larger drops grow at the expenses of the smaller drops and, thus, results in the change of the drop size distribution of the dispersions.

The model shows that the interdrop coalescence takes place faster than phase separation in the cream, which seems to agree well with experimental evidence. This will hold true as long as the capillary forces are greater than the gravitational forces. In actual practice, interdrop coalescence eventually leads to relatively large drops which push through the cream because of the large gravitational forces. At that stage the model will not be able to predict the coalescence within the cream.

Acknowledgment

This work was supported in part by the National Science Foundation, the Department of Energy and by Kraft General Foods.

Notation

a = radius of the cylindrical component of the deformed drop in a stack
 A_f = area of the film
 A'_f = area of the curved film projected normal to the line joining the centers of the drops
 b = $\Delta\rho g/\sigma$
 c^s = concentration of the surfactant in the bulk solution
 d = arithmetic mean drop diameter in the cream
 d_i = initial drop diameter ($t=0$)
 d_m = arithmetic mean drop diameter in the coalesced layers of the cream
 D = bulk diffusion coefficient of the surfactant
 D_s = surface diffusion coefficient of the surfactant
 F = force acting on the films
 g = acceleration due to gravity
 h = thickness of the film
 h_{cr} = critical thickness of film rupture
 H_{con} = height of the container
 H_{cr} = height of the cream
 i = power index in the coalescence equation
 j = power index in the sedimentation equation
 k = scaling factor for the rate of propagation of coalescence through the stack

m = number of coalescence steps that have occurred
 M = mobility factor in the film drainage equation to account for the presence of surfactant
 n = number of the original layers of drops in the stack, which have undergone coalescence. The layers are numbered from the bottom to the top in the initial stack ($t=0$)
 N = number of drops below a given drop within a vertical stack
 P_c = pressure jump across a curved surface (from the Laplace equation)
 P_f = pressure in the film
 P_r = excess pressure in the drop over that in the continuous phase
 R = radius of the film
 R_c = radius of the drop at its equator
 R'_c = radius of a spherical drop without any films
 R_d = radius of the spherical component of the deformed drop in a vertical stack
 R_f = radius of curvature of the film
 t = time
 t_{cr} = time for creaming to occur
 t_i = time period between the i th and $(i+1)$ th coalescence steps
 u_s = sedimentation velocity
 V = film drainage velocity in the presence of surfactant
 V_{RE} = Reynold's film drainage velocity
 w = buoyant weight of a drop = $4/3 \pi R_c'^3 \Delta\rho g$

Greek letters

α = angle made by the tangent to the curves surface of the drop and the horizontal
 Γ = surface concentration of the surfactant
 δP_c = change in the capillary pressure in a deformed drop = $P_c - P_g$
 ΔP = driving force for film drainage = P_g
 $\Delta\rho$ = density difference between the drop phase and the continuous phase
 ϵ_s = disperse phase holdup in the sedimentation zone
 ϵ_o = disperse phase holdup in the well mixed emulsion, before settling
 Θ = angle subtended by the arc of the curved film
 μ = viscosity of the continuous phase
 Π = disjoining pressure
 σ = interfacial tension between the drop phase and the continuous phase
 τ = lifetime of a film
 τ_1 = lifetime of the films between the bottom two rows of drop in the original stack
 τ_f = fractional decrease in the lifetime of an old film between two succeeding coalescence steps
 τ_m = lifetime of an old film after m coalescence steps
 τ_n = lifetime of a film formed between drops in the n th layer and the $(n+1)$ th of the initial stack ($t=0$)

Literature Cited

- Burill, A. K., and D. R. Woods, "Change in Interface and Film Shapes for a Deformable Drop at a Deformable Liquid-Liquid Interface I.," *J. Colloid Interface Sci.*, **30**, 511 (1969).
 Burill, A. K., and D. R. Woods, "Film Shapes for Deformable Drops at Liquid-Liquid Interfaces II. The Mechanism of Film Drainage," *J. Colloid Interface Sci.*, **42**, 15 (1973).
 Chakarova, S. K., M. Dupeyrat, E. Nakache, C. D. Dushkin, and I. B. Ivanov, "The Role of the Surfactant Distribution on the Lifetime of Drops in the System Water/Nitroethane," *J. Surface Sci. Technol.*, **6**, 17 (1990).
 Charles, G. E., and S. G. Mason, "The Coalescence of Liquid Drops with Flat Liquid-Liquid Interfaces," *J. Colloid Sci.*, **15**, 236 (1960).
 Frankel, S. P., and K. J. Mysels, "On the Dimpling During the Approach of Two Interfaces," *J. Phys. Chem.*, **66**, 191 (1962).
 Hartland, S., and R. Hartley, *Axisymmetric Fluid-Liquid Interfaces*, Elsevier Science Publishing Co., New York (1976).
 Hartland, S., and N. Gakis, "A Model for Coalescence in a Two-dimensional Close-Packed Dispersion," *Proc. R. Soc. Lond. A*, **369**, 137 (1979).
 Hartland, S., and D. K. Vohra, "Effect of Interdrop Forces on the

Coalescence of Drops in Close-Packed Dispersions," *J. Colloid Interface Sci.*, **77**, 295 (1980).

Hartland, S., and S. A. K. Jeelani, "Prediction of Steady-State Dispersion," *Chem. Eng. Sci.*, **42**, 1927 (1988a).

Hartland, S., and S. A. K. Jeelani, "Prediction of Sedimentation and Coalescence Profiles in a Decaying Batch Dispersion," *Chem. Eng. Sci.*, **43**, 2421 (1988).

Hartland, S., and K. K. Vohra, "Koaleszenz in Vertikalen Dichtgepackten Dispersionen," *Chem. Ing. Tech.*, **50**, 673 (1978).

Hodgson, T. D., and D. R. Woods, "The Effect of Surfactants on the Coalescence of a Drop at an Interface II," *J. Colloid Interface Sci.*, **30**, 429 (1969).

Ivanov, I. B., and T. T. Traykov, "Hydrodynamics of Thin Liquid Films. Rate of Thinning of Emulsion Films from Pure Liquids," *Int. J. Multiphase*, **2**, 397 (1976).

Ivanov, I. B., "Effect of Surface Mobility on the Dynamic Behavior of Thin Liquid Films," *Pure Appl. Chem.*, **52**, 1241 (1980).

Ivanov, I. B., D. S. Dimitrov, P. Somasundaran, and R. K. Jain, "Thinning of Films with Deformable Surfaces: Diffusion Controlled Surfactant Transfer," *Chem. Eng. Sci.*, **40**, 137 (1985).

Ivanov, I. B., and D. S. Dimitrov, "Thin Film Drainage," *Thin Liquid Films*, I. B. Ivanov (ed.), Marcel Dekker Inc., New York, p. 379 (1988).

Jeelani, S. A. K., and S. Hartland, "Prediction of Dispersion Height in Liquid-Liquid Gravity Settlers from Batch Settling Data," *AIChE J.*, **31**, 711 (1985).

Jeelani, S. A. K., A. Pandit, and S. Hartland, "Factors Affecting the Decay of Batch Liquid-Liquid Dispersions," *Can. J. Chem. Eng.*, **68**, 924 (1990).

Kumar, A., and S. Hartland, "Gravity Settling in Liquid-Liquid Dispersions," *Can. J. Chem. Eng.*, **63**, 368 (1985).

Maldarelli, C., and R. K. Jain, "Hydrodynamic Stability of Thin Films," *Thin Liquid Films*, I. B. Ivanov (ed.), Marcel Dekker Inc., New York, p. 497 (1988).

Malhotra, A. K., and D. T. Wasan, "Effects of Surfactant Adsorption-Desorption Kinetics and Interfacial Rheological Properties on the Rate of Drainage of Foam and Emulsion Films," *Chem. Eng. Comm.*, **55**, 95 (1987).

Menon, V. B., and D. T. Wasan, "Coalescence of Water-in-Shale Oil Emulsions," *Sep. Sci. Technol.*, **19**, 555 (1984).

Princen, H. M., "Gravitational Syneresis in Foams and Concentrated Emulsions," *J. Colloid Interface Sci.*, **34**, 188 (1980).

Princen, H. M., "Osmotic Pressure of Foams and Highly Concentrated Emulsions. 1. Theoretical Considerations," *Langmuir*, **2**, 519 (1986).

Princen, H. M., and A. D. Kiss, "Osmotic Pressure of Foams and Highly Concentrated Emulsions. 2. Determination from the Variation in Volume Fraction with Height in an Equilibrated Column," *Langmuir*, **3**, 36 (1987).

Reynolds, O., "On the Theory of Lubrication and its Applications Mr. Beauchamp Tower's Experiments, Including an Experimental Determination of the Viscosity of Olive Oil," *Phil. Trans. Roy. Soc. (London)*, **A177**, 157 (1886).

Scheludko, A., "Thin Liquid Films," *Adv. Colloid Interface Sci.*, **1**, 391 (1967).

Traykov, T. T., and I. B. Ivanov, "Hydrodynamics of Thin Liquid Films. Effect of Surfactants on the Velocity of Thinning of Emulsions Films," *Int. J. Multiphase Flow*, **3**, 471 (1977).

Vrij, A., "Possible Mechanism for the Spontaneous Rupture of Thin Free Liquid Films," *Discuss. Faraday Soc.*, **42**, 28 (1966).

Zapryanov, Z., A. K. Malhotra, N. Aderangi, and D. T. Wasan, "Emulsion Stability: An Analysis of the Effects of Bulk and Interfacial Properties on Film Mobility and Drainage Rate," *Int. J. Multiphase Flow*, **9**, 105 (1983).

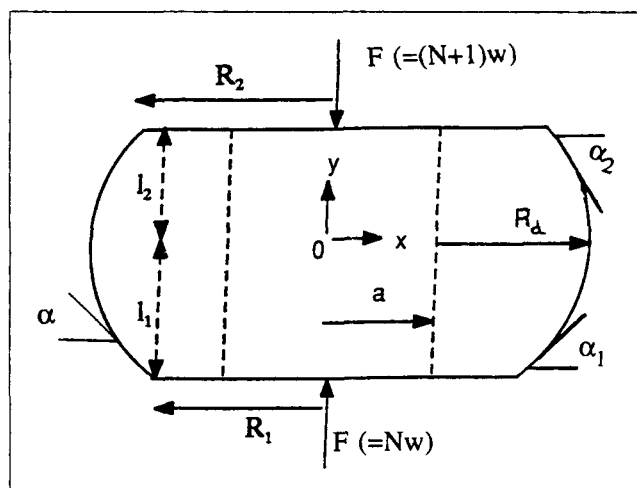


Figure A1. Deformation of a spherical drop due to applied force—constant volume assumption.

uated in two ways—(1) by determining the change in the capillary pressure when the condition of constant drop volume is imposed and (2) by determining the change in the drop volume when constant capillary pressure is assumed. In the first method, the condition for constant volume dictates that the drop shape deviate from sphericity. In this case, due to the force acting on the lower film of the drop and due to an opposing force on the upper film, the drop becomes barrel shaped, that is, it is assumed to be a composite of a truncated sphere of radius R_d and a cylinder of radius a , as shown in Figure A1.

Consider a vertical stack of monodisperse drops whose initial radii are R_c' (radius of the sphere before deformation). Consider a single drop, within the stack, with N drops below it. Since the volume of the deformed drop is assumed constant it must satisfy the condition:

$$V = \int_{-l_1}^{l_2} \pi \left(a^2 + R_d^2 - y^2 + 2a\sqrt{R_d^2 - y^2} \right) dy = \frac{4}{3} \pi R_c'^3 \quad (\text{A1})$$

where a , l_1 , l_2 and R_d are geometrical variables defined in Figure A1.

It is initially assumed that the capillary pressure within the deformed drop is the same as that in the nondeformed drop and the error of this assumption is evaluated later. By applying the force balance on the curved surfaces of the drop (exclude the film surface) one obtains:

$$P_g \pi (R_2^2 - R_1^2) = 2\pi\sigma [R_2 \sin \alpha_2 - R_1 \sin \alpha_1] \quad (\text{A2})$$

(see Figures A1 and A2 for definitions of α_1 and α_2)

The force balance on each of the films gives:

$$P_f \pi R_2^2 = (N+1)w \quad ; \quad P_f \pi R_1^2 = Nw \quad (\text{A3})$$

For given values of R_c' , σ , $\Delta\rho$ and N ; R_d and a can be determined. The above analysis satisfies the condition for the constancy of the volume of the drop. The actual capillary pressure is obtained from the Laplace equation for the drop surface (Hartland and Hartley, 1976):

Appendix

Calculating the deformation of a drop in a vertical stack

As mentioned earlier, the degree of deformation of a single drop which is present in a vertical stack of drops can be eval-

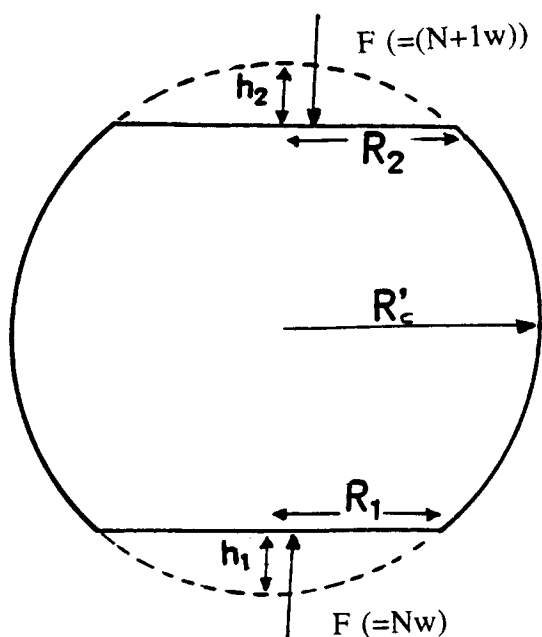


Figure A2. Truncated spherical drops due to films formed by applied force—constant capillary pressure assumption.

$$\frac{1}{x} \frac{d}{dx} (x \sin \alpha) = \frac{P_c}{\sigma} \quad (\text{A4})$$

where x is the value of the horizontal coordinate shown in Figure A1. The relation between x and α is given by:

$$x = a + R_d \cos \alpha \quad (\text{A5})$$

$\delta P_c = P_c - 2\sigma/R'_c$ represents the deviation in the capillary pressure due to deformation from sphericity and this deviation is found to be maximum at the equator ($y=0$) of the drop.

The second method that can be used to evaluate the extent of deformation is to assume the capillary pressure to be constant and then determine the change in the volume of the drop. Since the capillary pressure is assumed to be constant, the surfaces of the drop that do not form parts of the film remain as parts of the original sphere (truncated at both ends), as shown in Figure A2. The radii of the films on the drop are given, as before, by the relations in Eq. A3. The change in the volume of the drop δV is given by:

$$\delta V = \frac{1}{3} \pi h_1^2 (3R'_c - h_1) + \frac{1}{3} \pi h_2^2 (3R'_c - h_2) \quad (\text{A6})$$

where h_1 and h_2 are the dimensions shown in Figure A2.

Figures A3 and A4 shows the plots of δP_c (at $y=0$)/ P_c and $\delta V/V$ vs. $R_c'^2 b \sqrt{N}$. $R_c'^2 b \sqrt{N}$ represents the ratio of the force of deformation (due to gravity) to the capillary force. The deformation forces increase with the drop size, number of drops in the stack and the density difference between the two phases. The capillary forces increase with the increase in the interfacial tension and the decrease in the drop size. It is seen from the plots in Figures A3 and A4 that the error is quite small (<5%) for values of $R_c'^2 b \sqrt{N}$ up to 70. As an example,

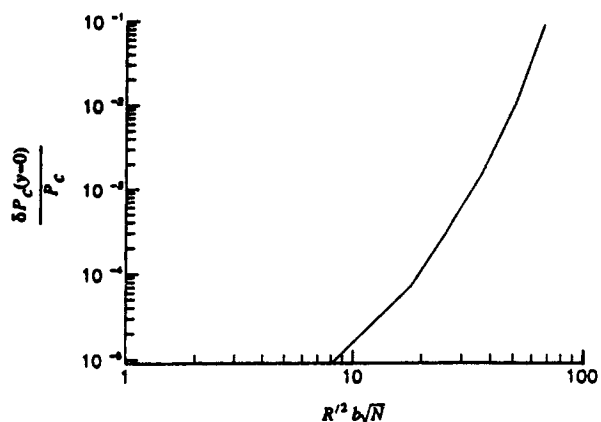


Figure A3. Change in capillary pressure due to deformation—constant volume assumption.

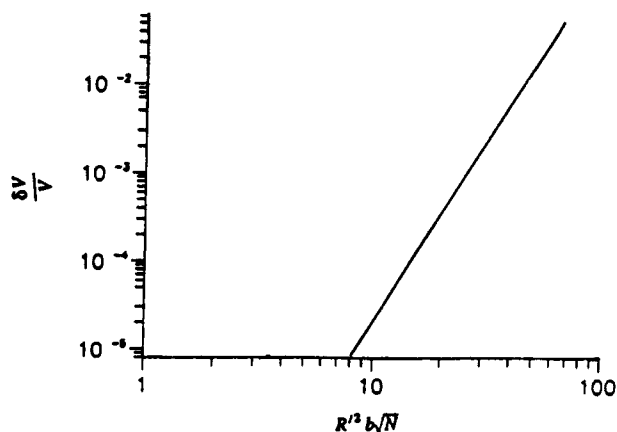


Figure A4. Change in drop volume due to deformation—constant capillary pressure assumption.

for drops of size $R'_c = 50 \mu\text{m}$ (which are fairly large), with a density difference of 0.2 g/cm^3 and an interfacial tension of 5 dyne/cm , the error due to deformation is less than 2% for $N = 1,200$ drops ($R_c'^2 b \sqrt{N} = 54.2$), which translates to approximately 6 cm of the height of the cream. Emulsions of interest to this study are expected to have deformations of the same order and this small deformation signifies that the capillary forces overshadow the gravitational forces. Since this deformation is evaluated to be small, the model neglects this effect, which signifies that the films are independent of each other. It is obvious that, as $R_c'^2 b \sqrt{N}$ increases, the gravitational forces may become important and the deformation cannot be neglected. This condition would arise if the interfacial tension is low, if the density difference is high or if the drop size is large, which is why the model cannot be used for foams.

The above analysis was done for the case when there are two films on the drop. As seen earlier, there are usually more than two films on each drop, and in this case a similar procedure can be applied. However, the errors in the capillary pressure or the volume depend on the total force acting on the drop and the size of the drop. Thus, if the same force which is acting on one film is redistributed to two films, these errors would remain the same.

Manuscript received March 30, 1992, and revision received Aug. 26, 1992.